FULL PAPER   *Pathology*

Gene Expression Profiling and Cellular Distribution of Molecules with Altered Expression in the Hippocampal CA1 Region after Developmental Exposure to Anti-Thyroid Agents in Rats

Yukie SAEGUSA[1,2)], Gye-Hyeong WOO[3)], Hitoshi FUJIMOTO[3)], Kaoru INOUE[3)], Miwa TAKAHASHI[3)], Masao HIROSE[3,4)], Katsuhide IGARASHI[5)], Jun KANNO[5)], Kunitoshi MITSUMORI[1)], Akiyoshi NISHIKAWA[3)] and Makoto SHIBUTANI[1)]*

[1)]Laboratory of Veterinary Pathology, Tokyo University of Agriculture and Technology, 3–5–8 Saiwai-cho, Fuchu-shi, Tokyo 183–8509, [2)]Pathogenetic Veterinary Science, United Graduate School of Veterinary Sciences, Gifu University, 1–1 Yanagido, Gifu-shi, Gifu 501–1193, [3)]Division of Pathology and [5)]Division of Molecular Toxicology, National Institute of Health Sciences, 1–18–1 Kamiyoga, Setagaya-ku, Tokyo 158–8501 and [4)]Food Safety Commission, Akasaka Park Bld. 22nd F., 5–2–20 Akasaka, Minato-ku, Tokyo 100–8989, Japan

ABSTRACT. To determine whether developmental hypothyroidism causes permanent disruption of neuronal development, we first performed a global gene expression profiling study targeting hippocampal CA1 neurons in male rats at the end of maternal exposure to anti-thyroid agents on weaning (postnatal day 20). As a result, genes associated with nervous system development, zinc ion binding, apoptosis and cell adhesion were commonly up- or down-regulated. Genes related to calcium ion binding were up-regulated and those for myelination were often down-regulated. We, then, examined immunohistochemical cellular distribution of Ephrin type A receptor 5 (EphA5) and Tachykinin receptor (Tacr)-3, those selected based on the gene expression profiles, in the hippocampal formation at the adult stage (11-week-old) as well as at the end of exposure. At weaning, both EphA5- and Tacr3-immunoreactive cells with strong intensities appeared in the pyramidal cell layer or stratum oriens of the hippocampal CA1 region. Although the magnitude of the change was decreased at the adult stage, Tacr3 in the CA1 region showed a sustained increase in expressing cells until the adult stage after developmental hypothyroidism. On the other hand, EphA5-expressing cells did not show sustained increase at the adult stage. The results suggest that developmental hypothyroidism caused sustained neuronal expression of Tacr3 in the hippocampal CA1 region, probably reflecting a neuroprotective mechanism for mismigration.

KEY WORDS: developmental hypothyroidism, EphA5, hippocampal CA1 region, Tacr3.

J. Vet. Med. Sci. 72(2): 187–195, 2010

Thyroid hormones are essential for normal fetal and neonatal brain development. They control neuronal and glial proliferation in definitive brain regions and regulate neural migration and differentiation [12, 18, 21]. In humans, maternal hypothyroxinemia, early in pregnancy, may have adverse effects on fetal brain development and importantly, even mild-moderate hypothyroxinemia may result in suboptimal neurodevelopment [4]. These results may increase the concern of thyroid hormone-disrupting chemicals in the environment.

Experimentally, developmental hypothyroidism leads to growth retardation, neurological defects and impaired performance on a variety of behavioral learning actions [1, 2]. Rat offspring exposed maternally to anti-thyroid agents such as 6-propyl-2-thiouracil (PTU) show brain retardation, with impaired neuronal migration and white matter hypoplasia involving limited axonal myelination and oligodendrocytic accumulation [6, 8, 21]. The outcome of this type of brain retardation is permanent and is accompanied by apparent structural and functional abnormalities. However, it is still unclear whether the molecular aberrations remain in the retarded brain after maturation.

Histological lesion-specific gene expression profiling provides valuable information on the mechanisms underlying lesion development. We have established molecular analysis methods for DNA, RNA and proteins in paraffin-embedded small tissue specimens utilizing an organic solvent-based fixative, methacarn, with high performance close to that achieved with unfixed frozen tissue specimens [22, 26, 27]. We have previously applied these techniques to analyze global gene expression changes in microdissected lesions [23, 28].

Hippocampal CA1 region is a well-known target of developmental hypothyroidism [8], and we, in our recent study, detected a distribution variability of hippocampal CA1 pyramidal neurons reflecting mismigration in rat offspring at the adult stage after developmental exposure to anti-thyroid agents [24]. The present study was performed to determine whether developmental hypothyroidism triggers sustained aberrations in neuronal development associated with neuronal mismigration until the adult stage. For this purpose, we first performed a global gene expression profiling of the CA1-pyramidal cell layer in rat offspring at the end of developmental exposure to anti-thyroid agents. To distinguish chemical-specific expression changes from hypothyroidism-linked ones, two different anti-thyroid

* CORRESPONDENCE TO: SHIBUTANI, M., Laboratory of Veterinary Pathology, Tokyo University of Agriculture and Technology, 3–5–8 Saiwai-cho, Fuchu-shi, Tokyo 183–8509, Japan.
  e-mail: mshibuta@cc.tuat.ac.jp

agents, PTU and 2-mercapto-1-methylimidazole (MMI), were used, and dose-related responses were also examined with PTU. To extract the neuronal cell layer-specific gene expression profile, microdissection technique was applied for microarray analysis. Based on the expression profiles obtained, cellular localization of the molecules showing altered expression were then immunohistochemically examined in the hippocampus at the adult stage as well as at the end of the developmental exposure.

MATERIALS AND METHODS

Chemicals and animals: 6-propyl-2-thiouracil (PTU; CAS No. 51–52–5) and methimazole (2-mercapto-1-meth-ylimidazole: MMI; CAS No. 60–56–0) were obtained from Sigma Chemical Co. (St. Louis, MO, U.S.A.). Pregnant Crj:CD®(SD)IGS rats were purchased from Charles River Japan Inc. (Yokohama, Japan) at gestation day (GD) 3 (appearance of vaginal plugs was designated as GD 0). Animals were housed individually in polycarbonate cages with wood chip bedding, maintained in an air-conditioned animal room (temperature: $24 \pm 1°C$; relative humidity: $55 \pm 5\%$) with a 12-hr light/dark cycle and allowed *ad libitum* access to food and tap water. A soy-free diet (Oriental Yeast Co., Ltd., Tokyo, Japan) was chosen as the basal diet for the maternal animals to eliminate possible phytoestrogen effects [10], and water was given *ad libitum* throughout the experimental period including the 1-week acclimation period.

Animal experiments: The animal experiments were identical to those in a previous study [24]. In brief, maternal animals were randomly divided into four groups including untreated controls. Eight dams per group were treated with 3 or 12 ppm of PTU or 200 ppm of MMI in the drinking water from GD 10 to postnatal day (PND) 20 (PND 0: the day of delivery). On PND 2, the litters were culled randomly, leaving four male and four female offspring. On PND 20, 20 male and 20 female offspring (at least one male and one female per dam) per group were subjected to prepubertal necropsy [13, 24].

The remaining animals were maintained until postnatal week (PNW) 11. All offspring consumed the CRF-1 basal diet and tap water *ad libitum* from PND 21 onwards. At PNW 11, all pups were subjected to adult stage necropsy [13, 24].

All animals used in the present study were weighed and sacrificed by exsanguination from the abdominal aorta under deep anesthesia. These protocols were reviewed in terms of animal welfare and approved by the Animal Care and Use Committee of the National Institute of Health Sciences, Japan.

Preparation of tissue specimens and microdissection: For microarray and subsequent real-time RT-PCR analyses, the whole brain of male offspring was removed at prepubertal necropsy on PND 20 (n=4/group) and was fixed with meth-acarn solution for 2 hr at 4°C [22]. Coronal brain slices taken at the position of –3.5 mm from the bregma were

dehydrated and embedded in paraffin. The embedded tissue blocks were stored at 4°C until tissue sectioning for micro-dissection [9].

For microdissection, 4-μm-thick sections between ten 20 μm-thick serial sections were prepared. The 4 μm-thick sections were stained with hematoxylin and eosin for confirmation of anatomical orientation of the hippocampal sub-structure to aid microdissection. The 20 μm-thick sections were mounted onto PEN-foil film (Leica Microsystems GmbH, Welzlar, Germany) overlaid on glass slides, dried in an incubator overnight at 37°C, and then stained using an LCM staining kit (Ambion, Inc., Austin, TX, U.S.A.). Bilateral sides of the hippocampal CA1 pyramidal cell layer in the sections were subjected to laser microbeam microdis-section (Leica Microsystems GmbH) (Fig. 1). Twenty sections from each animal were used for microdissection, and the bilateral microdissected samples were collected and stored in separate 1.5-m*l* sample tubes at –80°C until the extraction of total RNA.

RNA preparation, amplification and microarray analysis: Total RNA extraction from hippocampal CA1 samples, quantitation of the RNA yield, and amplification of RNA samples were performed using previously described methods [9, 28].

For microarray analysis, second-round-amplified biotin-labeled antisense RNAs were subjected to hybridization with a GeneChip® Rat Genome 230 2.0 Array (Affymetrix, Inc., Santa Clara, CA, U.S.A.), as previously described [28].

The selection of genes and normalization of the expression data were performed using GeneSpring® software (ver7.2, Silicon Genetics, Redwood City, CA, U.S.A.). Per chip normalization was performed according to a previously described method [28]. Genes showing signals judged to be "absent" in all eight samples of untreated controls and in the anti-thyroid agent-exposed group were excluded. Genes
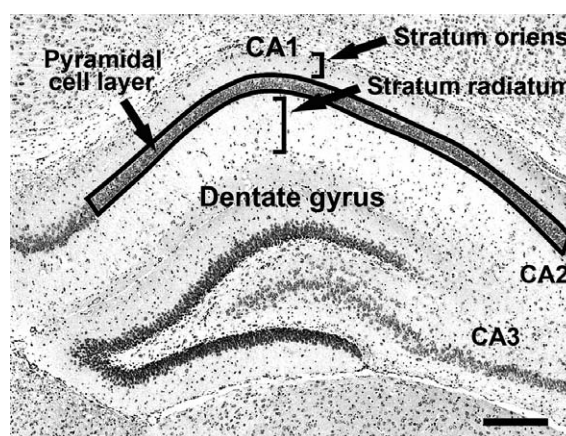

Fig. 1. Overview of the hippocampal formation of a male rat at postnatal day 20 stained with hematoxylin and eosin. Bar=200 μm. The CA1 pyramidal cell layer, enclosed by a solid line, was microdissected for the microarray and subsequent real-time RT-PCR analyses. The number of cells immunoreactive for the candidate molecules in this area was normalized for the length of CA1 used.

showing expression changes with differences of at least twofold in magnitude from the untreated controls were selected, and the "presence" signal in more than 3/4 of samples in each group showing higher expression values were selected. Genes showing altered expression in common in the anti-thyroid agent-exposed groups were also selected.

Real-time RT-PCR: Quantitative real-time RT-PCR was performed to confirm the expression values obtained with microarrays using an ABI Prism 7000 Sequence Detection System (Applied Biosystems Japan, Tokyo, Japan). Genes those showing altered expression (≥2-fold, ≤0.5-fold) in common in the anti-thyroid agent-exposed groups as compared with untreated control offspring were randomly selected, irrespective of the presence or absence of statistically significant difference. As a result, the following seven genes (four up-regulated and three down-regulated) with known function were selected as targets: Tachykinin receptor 3 (*Tacr3*), Calbindin 1, Slit homolog 2 (Drosophila) and Pleomorphic adenoma gene-like 1 (*Plagl1*) as up-regulated examples, and Myelin-associated oligodendrocytic basic protein (*Mobp*), Endothelial differentiation, sphingolipid G-protein-coupled receptor, 8 and CCAAT/enhancer binding protein as down-regulated. RT was performed using first-round antisense RNAs prepared for microarray analysis. For real-time PCR analysis of the genes selected, ABI Assays-on-Demand™ TaqMan® probe and primer sets from Applied Biosystems (available at https://products.applied biosystems.com/ab/en/US/adirect/ab?cmd=catNavigate2 &catID=601267)(n=4/group) were used. For quantification of the expression data, a standard curve method was applied. The expression values were normalized to two housekeeping genes, Glyceraldehyde 3-phosphate dehydrogenase and Hypoxanthine-guanine phosphoribosyltransferase.

Immunohistochemistry: To evaluate the immunohistochemical distribution of the molecules selected by microarray analysis, the brains of male pups obtained at PND 20 or PNW 11 were fixed in Bouin's solution at room temperature overnight. Six animals were used as untreated controls, six for 200 ppm MMI, eight for 3 ppm PTU, and nine for 12 ppm PTU on PND 20. On PNW 11, 10 animals were used as untreated controls and 10 for 200 ppm MMI, nine for 3 ppm PTU, and six for 12 ppm PTU.

Immunohistochemistry was performed on the brain tissue sections of PND 20 and PNW 11 animals with antibodies against Ephrin type A receptor 5 (EphA5; rabbit IgG, 1:50; Abcam, Cambridge, U.K.) and Tacr3 (rabbit polyclonal antibody, 1:3,000, Novus Biologicals, Inc., Littleton, CO, U.S.A.), which were incubated with the tissue sections overnight at 4°C. Antigen retrieval treatment was not performed for these antigens. Immunodetection was carried out using a VECTASTAIN® Elite ABC kit (Vector Laboratories Inc., Burlingame, CA, U.S.A.) with 3,3'-diaminobenzidine/H_2O_2 as the chromogen, as previously described [23]. The sections were then counterstained with hematoxylin and coverslipped for microscopic examination.

With regard to EphA5, *Efna5*, a gene encoding the representative ligand for this receptor molecule [5], was found to be up-regulated (≥2-fold) by microarray analysis in all of the groups exposed to anti-thyroid agents in the present study (Table 1). Because distribution of EphA5 has been confirmed in the pyramidal cells of the hippocampal CA1 region at both developmental and adult stages in mice and at adult stage in humans [3, 17], we selected this molecule to examine distribution changes in the present study. Tacr3 was also up-regulated in all of the MMI and PTU groups by microarray analysis and real-time RT-PCR in the present study (Table 1). Expression of Tacr3 in the hippocampal CA1 pyramidal neurons has also been confirmed in rats [11], and therefore, we also selected this molecule for examination in the expression changes in the present study.

Morphometry of immunolocalized cells and apoptotic cells: EphA5- or Tacr3-immunoreactive cells distributed in the pyramidal cell layer or stratum oriens of the hippocampal CA1 region were bilaterally counted and normalized to the number in the length of the CA1 region measured (Fig. 1). Tacr3-immunoreactive cells in the subgranular zone of the dentate gyrus were also bilaterally counted and normalized for the number in the length of the granular zone measured. For quantitative measurement of each immunoreactive cellular component, digital photomicrographs at 100-fold magnification were taken using a BX51 microscope (Olympus Optical Co., Ltd., Tokyo, Japan) attached to a DP70 Digital Camera System (Olympus Optical Co., Ltd.), and quantitative measurements were performed using the WinROOF image analysis software package (version 5.7, Mitani Corp., Fukui, Japan).

Statistical analysis: Numerical data of the number of immunoreactive cells were assessed using Student's *t*-test to compare the untreated controls with each of the anti-thyroid agent-exposed groups when the variance was homogenous among the groups using a test for equal variance. If a significant difference in variance was observed, Aspin-Welch's *t*-test was used instead. The data for gene expression levels from real-time RT-PCR analysis were analyzed by the Kruskal-Wallis test, followed by Bartlett's test. When statistically significant differences were indicated, Dunnett's multiple test was used for comparisons with the untreated controls. For the microarray data, statistical analysis was performed with GeneSpring® software, and the significance of gene expression changes was analyzed by Student's *t*-test or ANOVA between the untreated controls and each of the anti-thyroid agent-exposed groups.

RESULTS

Microarray analysis: Figure 2 shows the Venn diagram of genes showing altered expression in the microdissected CA1 pyramidal neurons in the exposure groups in combination or individually in each exposure group. Many genes were found to be up- or down-regulated in common in two of the three groups. The numbers of genes classified into common categories between the groups or individually in each group were similar in terms of up- and down-regulated genes. The number of genes showing up- or down-regula-

Table 1.   List of representative genes showing up- or down-regulation common to 2-mercapto-1-methylimidazole (MMI), 3 and 12 ppm 6-propyl-2-thiouracil (PTU) (≥2-fold, ≤0.5-fold)

Gene function	Accession No.	Gene title	Symbol	MMI	3 ppm PTU	12 ppm PTU
Up-regulated genes (of 119 genes in total)						
Nervous system development	AI101660	Slit homolog 2 (Drosophila)	Slit2	3.04	2.62	7.08
Nervous system development	NM_024358.1	Notch gene homolog 2 (Drosophila)	Notch2	2.52	2.01	2.02
Nervous system development	AW527295	Ephrin A5	Efna5	3.12	3.46	4.31
Nervous system development	NM_053465.1	Fucosyltransferase 9	Fut9	2.13	6.75	2.11
Nervous system development	BE106256	Sparc/osteonectin, cwcv and kazal-like domains proteoglycan 1	Spock1	3.22	3.13	2.15
Calcium ion binding	X04280.1	Calbindin 1	Calb1	4.48	4.85	9.00
Calcium ion binding	BM386119	UDP-N-acetyl-alpha-D-galactosamine:polypeptide N-acetylgalactosaminyltransferase 3 (GalNAc-T3)	Galnt3	2.43	2.30	2.63
Calcium ion binding	BI279663	Desmocollin 2	Dsc2	2.82	2.04	5.62
Calcium ion binding	AI105369	Calmodulin-like 4	Calml4	3.40	2.25	5.59
Zinc ion binding	BE098686	Similar to Tnf receptor-associated factor 1	LOC687813	3.10	2.04	2.78
Zinc ion binding	BF562032	RAN binding protein 2	Ranbp2	3.49	2.67	2.78
Zinc ion binding	BF397925	ADAMTS-like 1	Adamtsl1	6.22	2.55	7.63
Zinc ion binding	BF395606	Splicing factor, arginine/serine-rich 7	Sfrs7	4.93	2.06	2.90
Apoptosis	NM_012760.1	Pleomorphic adenoma gene-like 1	Plagl1	3.10	4.28	6.86
Apoptosis	NM_057130.1	Harakiri, BCL2 interacting protein (contains only BH3 domain)	Hrk	2.63	2.73	3.18
Cell Adhesion	AA850909	Poliovirus receptor-related 2	Pvrl2	4.74	2.46	2.61
Cell Adhesion	AA819731	Hyaluronan and proteoglycan link protein 4	Hapln4	4.13	6.67	3.46
Cell Adhesion	BI287851	Collagen, type VI, alpha 2	Col6a2	3.45	2.19	5.12
Ion channel activity	AA851939	FXYD domain-containing ion transport regulator 6	Fxyd6	4.73	2.61	7.85
Other	NM_017053.1	Tachykinin receptor 3	Tacr3	7.32	6.19	12.49
Down-regulated genes (of 97 genes in total)						
Nervous system development	NM_031018.1	Activating transcription factor 2	Atf2	0.41	0.36	0.36
Neuron migration	BF390065	Roundabout homolog 3 (Drosophila)	Robo3	0.06	0.31	0.04
Neuron differentiation	AF115249.1	Endothelial differentiation, sphingolipid G-protein-coupled receptor, 8	Edg8	0.40	0.06	0.08
Neuron differentiation	NM_024125.1	CCAAT/enhancer binding protein (C/EBP), beta	Cebpb	0.31	0.43	0.26
Myelination	X89638.1	Myelin-associated oligodendrocytic basic protein	Mobp	0.35	0.18	0.12
Myelination	NM_017190.1	Myelin-associated glycoprotein	Mag	0.47	0.36	0.29
Myelination	NM_022668.1	Myelin oligodendrocyte glycoprotein	Mog	0.44	0.32	0.19
Myelination	NM_012798.1	Mal, T-cell differentiation protein	Mal	0.37	0.28	0.28
Myelination	AA945178	Signal recognition particle receptor, B subunit transferrin	Srprb Tf	0.33	0.27	0.15
Zinc ion binding	NM_012566.1	Growth factor independent 1 transcription repressor	Gfi1	0.20	0.44	0.41
Zinc ion binding	AW529624	Zinc finger protein 91	Zfp91	0.33	0.32	0.38
Actin binding	AW522439	Ermin, ERM-like protein	Ermn	0.43	0.42	0.28
Apoptosis	BG377720	Solute carrier family 5 (sodium/glucose cotransporter), member 11	Slc5a11	0.25	0.19	0.19
Apoptosis	U21955.1	Eph receptor A	Epha7	0.34	0.48	0.18
Cell Adhesion	BM391100	Mucin 4, cell surface associated	Muc4	0.43	0.36	0.27
Other	AW435010	Protein tyrosine phosphatase, non-receptor type 3	Ptpn3	0.38	0.46	0.36
Other	AF312319.1	gamma-aminobutyric acid (GABA) B receptor 1	Gabbr1	0.33	0.41	0.39
Other	NM_053936.1	Endothelial differentiation, lysophosphatidic acid G-protein-coupled receptor, 2	Edg2	0.47	0.31	0.31

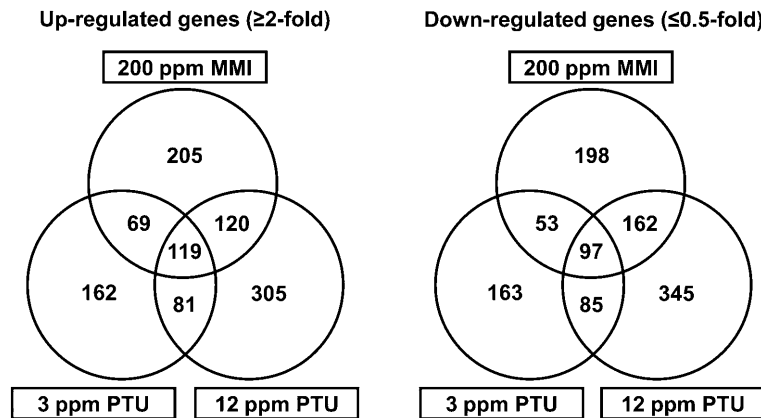**Up-regulated genes (≥2-fold)**   **Down-regulated genes (≤0.5-fold)**

Fig. 2.   Venn diagram of gene populations showing altered expression in the hippocampal CA1 pyramidal cell layer at postnatal day 20 in response to maternal exposure to propylthiouracil and/or 2-mercapto-1-methylimidazole compared with the untreated controls. (Left) Up-regulated genes (≥2-fold). (Right) Down-regulated genes (≤0.5-fold). Abbreviations: MMI, 2-mercapto-1-methylimidazole; PTU, 6-propyl-2-thiouracil.

Table 2.   Validation of microarray data by real-time RT-PCR

Gene	200 ppm MMI			3 ppm PTU			12 ppm PTU		
	Microarray	Real-time RT-PCR normalized to		Microarray	Real-time RT-PCR normalized to		Microarray	Real-time RT-PCR normalized to	
		Hprt[a]	Gapdh[b]		Hprt	Gapdh		Hprt	Gapdh
Tacr3[c]	7.32 ± 2.21**	4.29 ± 1.27	4.08 ± 1.15*	6.19 ± 2.19**	3.46 ± 1.42	3.76 ± 1.51*	12.49 ± 1.56**	9.23 ± 3.00**	8.81 ± 1.60**
Calb1[d]	4.48 ± 0.66*	3.96 ± 0.74	3.67 ± 0.16	4.85 ± 2.53*	4.74 ± 2.48	4.93 ± 3.79	9.00 ± 1.85**	11.13 ± 2.13**	10.53 ± 3.26**
Slit2[e]	3.04 ± 0.79	2.83 ± 0.90	4.08 ± 1.15*	2.62 ± 1.16	1.33 ± 0.67	3.67 ± 1.51*	7.08 ± 2.15**	4.72 ± 2.57**	8.81 ± 1.60**
Plgl1[f]	3.10 ± 1.57	12.67 ± 5.00	11.5 ± 7.50	4.28 ± 2.88	18.33 ± 6.00	19.00 ± 9.00*	6.86 ± 2.85**	30.67 ± 5.33**	27.00 ± 8.00**
Mobp[g]	0.35 ± 0.15**	0.6 ± 0.22*	0.52 ± 0.16**	0.18 ± 0.07**	0.24 ± 0.07**	0.24 ± 0.05**	0.12 ± 0.02**	0.18 ± 0.04**	0.16 ± 0.04**
Edg8[h]	0.40 ± 0.11*	0.49 ± 0.16*	0.43 ± 0.13*	0.06 ± 0.05**	0.29 ± 0.10**	0.28 ± 0.08**	0.08 ± 0.07**	0.21 ± 0.07**	0.18 ± 0.03**
Cebpb[i]	0.31 ± 0.06**	0.43 ± 0.04**	0.38 ± 0.06**	0.43 ± 0.18**	0.77 ± 0.07	0.76 ± 0.10	0.26 ± 0.04**	0.39 ± 0.16**	0.35 ± 0.22**

a) Hprt, Hypoxanthine-guanine phosphoribosyltransferase; b) Gapdh, Glyceraldehyde 3-phosphate dehydrogenase; c) Tacr3, Tachykinin receptor 3; d) Calb1, Calbindin 1; e) Slit2, Slit homolog 2 (Drosophila); f) Plgl1, Pleomorphic adenoma gene-like 1; g) Mobp, Myelin-associated oligodendrocytic basic protein; h) Edg8, Endothelial differentiation, sphingolipid G-protein-coupled receptor, 8; i) Cebpb, CCAAT/enhancer binding protein (C/EBP), beta.
Values are mean ± SD (n=4) relative to the expression level in the untreated controls. Real-time RT-PCR analysis of Hprt and Gapdh was performed in the analysis of each target gene.
*, **: Significantly different from the untreated controls at $P<0.05$ and $P<0.01$, respectively (Dunnett's multiple comparison test).

tion in response to 12 ppm PTU was approximately 2-fold higher than that with 3 ppm PTU. The number of genes showing up- or down-regulation in response to 200 ppm MMI was in between that elicited by 3 or 12 ppm PTU. One-hundred nineteen genes were up-regulated in common by MMI and PTU, with PTU showing up-regulation from 3 ppm. On the other hand, 97 genes showed down-regulation in all MMI and PTU groups. Representative genes showing up- or down-regulation in all three groups are shown in the Table 1. Among the genes listed, genes associated with nervous system development, zinc ion binding, apoptosis and cell adhesion were commonly up- or down-regulated. Genes related to calcium ion binding were found to be up-regulated and those for myelination were often down-regulated.

Real-time RT-PCR analysis: For confirmation of the microarray data, four genes that were up-regulated and three that were down-regulated in response to anti-thyroid agents were selected for mRNA expression analysis by real-time RT-PCR and the results are summarized in Table 2.

In all exposure groups, many of the expression changes were similar in the two analysis systems, except for much higher expression of *Plagl1* in all exposure groups by real-time RT-PCR as compared with findings from the microarray system.

Although we performed expression analysis of *Efna5* by real-time RT-PCR, expression values were rather low with great variability between samples, and therefore, reliable quantitative data could not be obtained (data not shown).

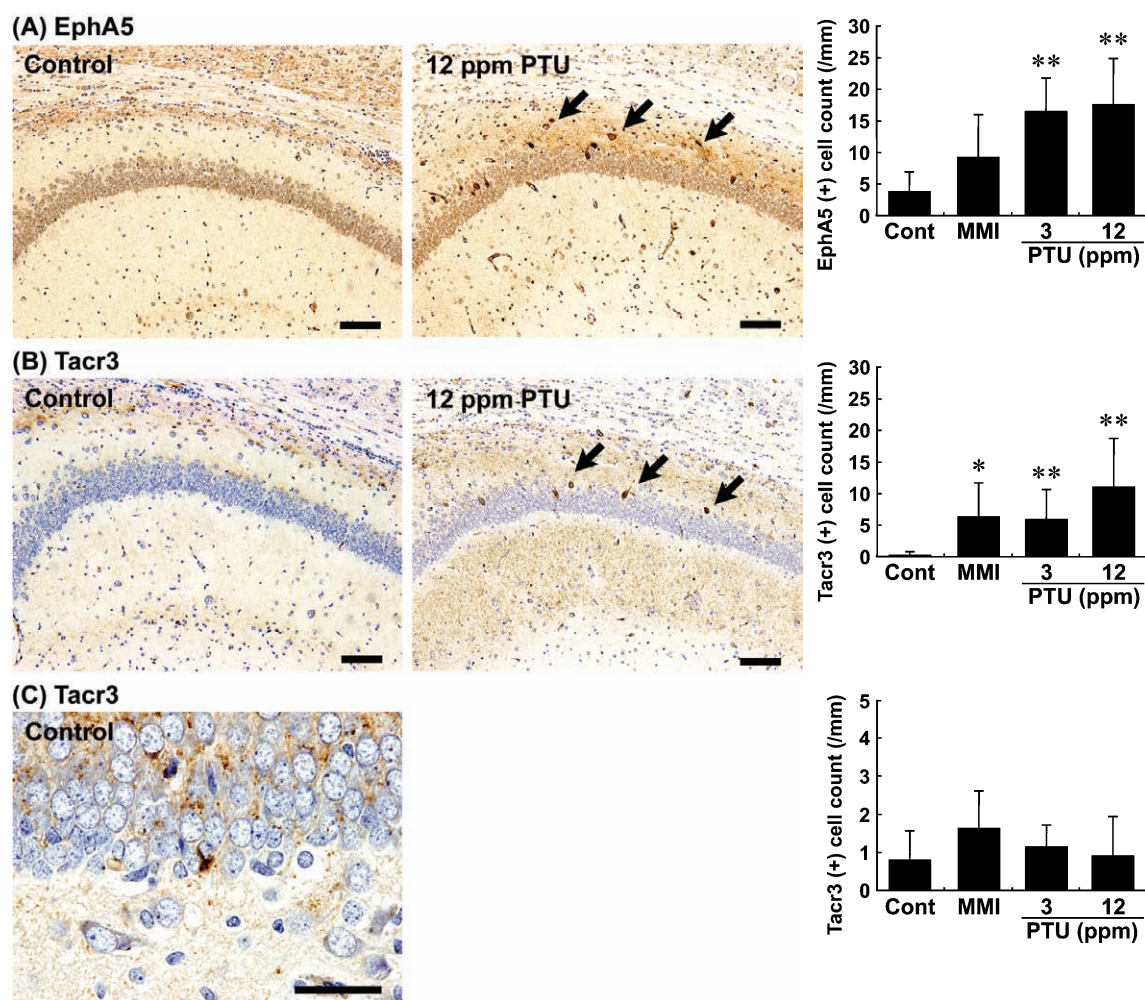*Immunolocalization of EphA5 and Tacr3 in the hippoc-*

Fig. 3. Distribution of immunoreactive cells for EphA5 and Tacr3 in the hippocampal formation in rats at PND 20 after maternal exposure to anti-thyroid agents. (A) EphA5-immunoreactive cells with strong intensity located within the pyramidal cell layer and stratum oriens of the hippocampal CA1 region (arrows). Note the higher number of EphA5-positive cells in a case exposed to 12 ppm PTU (Right) as compared with the control animal (Left). Bar =100 μm. The graph shows the number of EphA5-positive cells/unit length (mm) of the CA1 region of the bilateral hemispheres. ** $P<0.01$ versus untreated controls (Student's *t*-test). (B) Tacr3-immunoreactive cells with strong intensity located within the pyramidal cell layer and stratum oriens of the hippocampal CA1 region (arrows). Note the higher number of Tacr3-positive cells in a case exposed to 12 ppm PTU (Right) as compared with the control animal (Left). Bar =100 μm. The graph shows the number of Tacr3-positive cells/unit length (mm) of the CA1 region of bilateral hemispheres. * $P<0.05$, ** $P<0.01$ versus untreated controls (Student's *t*-test). (C) Tacr3-immunoreactive cells located in the subgranular zone of the dentate gyrus. Bar =50 μm. The graph shows the number of Tacr3-positive cells/unit length (mm) of the subgranular zone of bilateral hemispheres. Abbreviations: EphA5, Ephrin type A receptor 5; MMI, 2-mercapto-1-methylimidazole; PTU, 6-propyl-2-thiouracil, Tacr3, Tachykinin receptor 3.

ampal formation: Immunohistochemical localization of EphA5 and Tacr3 in the hippocampal formation was examined at PND 20 and PNW 11.

On PND 20, EphA5 showed weak immunoreactivity in the pyramidal neurons throughout the hippocampal formation in the untreated controls. This immunoreactivity was unchanged by exposure to anti-thyroid agents. On the other hand, very sparse distribution of strongly immunoreactive cells for EphA5 was observed in the region of the CA1 pyramidal cell layer and stratum oriens in the untreated control

animals, but immunoreactive cells were significantly increased showing scattered distribution by PTU at both 3 and 12 ppm (Fig. 3A). MMI-exposed animals also showed a small increase in the number of strongly positive cells with EphA5. Increased intensity in immunoreactivity of EphA5 was also observed in the gray matter consisting of neuropil at the stratum oriens of the CA1 region (Fig. 3A), and also in the molecular layer of the dentate gyrus at PND 20 after exposure to anti-thyroid agents, especially in PTU-exposed groups (data not shown).
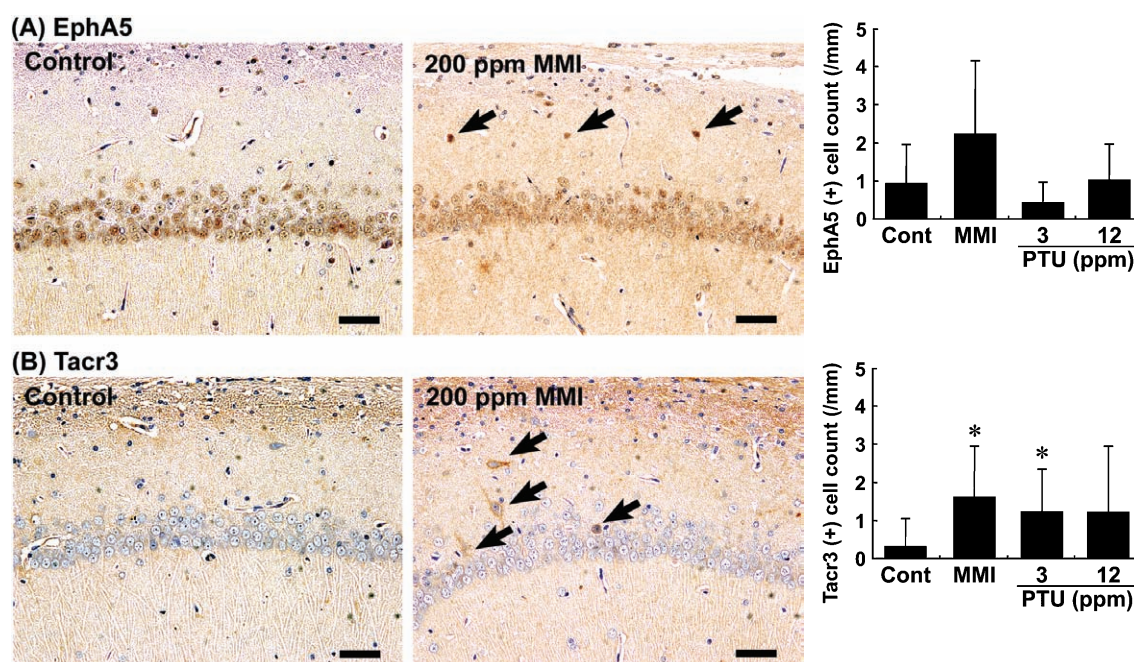
Fig. 4. Distribution of immunoreactive cells for EphA5 and Tacr3 in the hippocampal formation at PNW 11 of rats exposed maternally to anti-thyroid agents. (A) EphA5-immunoreactive cells with moderate staining intensity located within the pyramidal cell layer and stratum oriens of the hippocampal CA1 region. EphA5-positive cells in a case exposed to 200 ppm MMI (Right) as compared with the control animal (Left). The arrows show positive cells. Bar =50 μm. The graph shows the number of EphA5-positive cells/unit length (mm) of the CA1 region of the bilateral hemispheres. (B) Tacr3-immunoreactive cells with weak to moderate staining intensity located within the pyramidal cell layer and stratum oriens of the hippocampal CA1 region (arrows). Immunoreactivity is rather faint as compared with that observed at PND 20. Note the higher number of Tacr3-positive cells in a case exposed to 200 ppm MMI (Right) as compared with the control animal (Left). Bar =50 μm. The graph shows the number of Tacr3-positive cells/unit length (mm) of the CA1 region of bilateral hemispheres. * P<0.05 versus untreated controls (Student's t-test). Abbreviations: EphA5, Ephrin type A receptor 5; MMI, 2-mercapto-1-methylimidazole; PTU, 6-propyl-2-thiouracil; Tacr3, Tachykinin receptor 3.

With regards to Tacr3, the number of positive cells was increased with a scattered distribution showing strong intensity in the CA1 region similarly to that of EphA5 in the animals exposed to MMI or PTU on PND 20, but they were mostly absent in the untreated controls (Fig. 3B). Similarly, Tacr3-immunoreactive cells were sparse in the subgranular zone of the dentate gyrus in the MMI and PTU-exposed animals and in the untreated controls, but there were no differences in the number of positive cells as compared with the untreated controls (Fig. 3C). In addition, increased intensity in neuropil-immunoreactivity of Tacr3 was also observed in the strata oriens and radiatum of the CA1 region in all exposure groups of anti-thyroid agents (Fig. 3B).

On PNW 11, EphA5 showed weak immunoreactivity in the pyramidal neurons throughout the hippocampal formation in the untreated controls. This immunoreactivity was unchanged by exposure to anti-thyroid agents. EphA5-immunoreactive cells with moderate staining intensity were very sparsely observed in the region of the CA1 pyramidal cell layer and stratum oriens in the untreated control animals. There was no statistically significant increase in the number of these immunoreactive cells after exposure to PTU, while animals exposed to MMI showed a tendency for an increased number of immunoreactive cells (Fig. 4A). Increased neuropil-immunoreactivity of EphA5 as observed at PND 20 in exposure groups of anti-thyroid agents was mostly disappeared at PNW 11 (data not shown).

As well as at PND 20, Tacr3-immunoreactive cells were mostly absent in the untreated controls at PNW 11; however, a few immunoreactive cells with weak to moderate intensity were observed in the stratum oriens of the CA1 region in the animals exposed to anti-thyroid agents. There was a statistically significant difference in the animals treated with MMI or 3 ppm PTU compared with the untreated controls (Fig. 4B). Although the change was nonsignificant and lacked dose-dependence, 12 ppm PTU also showed an increasing tendency in the number of Tacr3-immunoreactive cells. In addition, increased neuropil-immunoreactivity of Tacr3 as observed at PND 20 in exposure groups of anti-thyroid agents was mostly disappeared at PNW 11 (data not shown).

DISCUSSION

In our recent study using rats [24], after maternal exposure to MMI or PTU, we detected typical hypothyroidism-related changes in the thyroid-related hormone levels, and hippocampal CA1 pyramidal neurons due to neuronal mismigration, as previously reported [8]. We also observed white matter changes, which seem to be due to impaired oligodendroglial development [6, 21]. To visualize molecules related to impaired neuronal development, microdissected CA1 region-specific global gene expression profiling was performed in the present study using the same animals that were used in our previous study. Two recently published studies have used microarrays to examine the expression profiles in the cerebral cortex and hippocampus of genes linked to developmental hypothyroidism caused by maternal PTU-exposure [7, 19]. In accordance with these studies, the genes that were significantly down-regulated in the present study included those that play roles in myelination, such as *Mobp* and myelin-associated glycoprotein, suggestive of the reflection of suppressed myelination by developmental hypothyroidism [21]. However, the genes that were found to be up-regulated on microdissected CA1 pyramidal cell layer, including *Efna5* and *Tacr3*, in the present study, have not been identified in previous studies. This difference may be related to the target tissues collected and the methods used, including microdissection of CA1 pyramidal cell layer from paraffin-embedded sections in the present study versus manual dissection of the cortical tissues from unfixed tissues in the previous studies.

EphA5 is a tyrosine kinase receptor that is almost exclusively expressed in the nervous system [15]. EphA5 and its ligand are important in mediating axon guidance, topographic projection, development, cell migration and the plasticity of limbic structures [15]. In addition, the transient expression of EphA5 during development is correlated with early neurogenesis and the migration of differentiated cells in the midbrain [3]. Thus, although expression of EphA5 was mostly weak in the euthyroid CA1 pyramidal neurons at PND 20, the increased number of EphA5-expressing cells with strong intensity in the CA1 region during developmental hypothyroidism in the present study reflects the neuronal mismigration caused by anti-thyroid agents. However, this increase was recovered after cessation of developmental hypothyroidism. Ephrins and their receptors are recently identified molecules and functional relationship between subfamily proteins is largely unknown; however, we, in the present study, found down-regulation of Epha7, another subfamily ephrin receptor, in all exposure groups of anti-thyroid agents (Table 1).

Tacr3, a member of the mammalian tachykinin peptide neurotransmitter/neuromodulator receptor family, is predominantly expressed in neurons in both the peripheral and central nervous systems, including the hippocampus [25]. There is increasing evidence of the role of Tacr3 on the survival and function of dopaminergic neurons. The survival of mesencephalic dopaminergic neurons during develop-

ment largely depends on excitatory inputs, and tachykinins, through their receptors, are reported to play role in excitation [20]. On the other hand, senktide, a Tacr3 agonist, activates dopaminergic neurons to stimulate the release of dopamine and serotonin, and hyperlocomotion in gerbils [14]. Abnormal excitatory action of D_2-like receptor, one of the major subtypes of dopaminergic receptors, was observed on glutamatergic transmission in the CA1 synapses in the adult stage of rats after developmental hypothyroidism, suggesting a permanent disruption of synaptic integration in the CA1 neural networks [16]. While the role of Tacr3 in the hippocampal CA1 region during development is not clear, the increase in Tacr3-positive cells with strong intensity in this region during developmental hypothyroidism suggests a cell survival effect of tachykinin-3. Although the magnitude of the change was decreased, as compared with that at the end of the developmental hypothyroidism, the increased number of Tacr3-positive cells in the CA1 region of MMI and 3 ppm PTU-exposed animals may be an outcome of permanent disruption of synaptic integration, as described by Oh-Nishi *et al.* [16]. However, sparse distribution of Tacr3-positive cells may reflect that impairment sustained in a small population of aberrantly migrated neurons.

In conclusion, in this study, we have shown gene expression profiles showing altered expression in response to developmental hypothyroidism by analysis on microdissected hippocampal CA1 pyramidal cell layer in rats. Immunohistochemical analysis of the two candidate molecules revealed that developmental hypothyroidism until weaning is associated with the persistence of Tacr3-expressing neurons until the adult stage in the CA1 region, suggestive of the reflection of permanent disruption of synaptic integration. These findings probably reflect a mechanism to facilitate cell survival of aberrantly developed neurons due to mismigration.

REFERENCES

1. Akaike, M., Kato, N., Ohno, H. and Kobayashi, T. 1991. Hyperactivity and spatial maze learning impairment of adult rats with temporary neonatal hypothyroidism. *Neurotoxicol. Teratol.* **13**: 317–322.
2. Comer, C. P. and Norton, S. 1982. Effects of perinatal methimazole exposure on a developmental test battery for neurobehavioral toxicity in rats. *Toxicol. Appl. Pharmacol.* **63**: 133–141.
3. Cooper, M. A., Crockett, D. P., Nowakowski, R. S., Gale, N. W. and Zhou, R. 2009. Distribution of EphA5 receptor protein

in the developing and adult mouse nervous system. *J. Comp. Neurol.* **514**: 310–328.

4. de Escobar, G. M., Obregón, M. J. and del Rey, F. E. 2007. Iodine deficiency and brain development in the first half of pregnancy. *Public Health Nutr.* **10**: 1554–1570.

5. Gerlai, R., Shinsky, N., Shih, A., Williams, P., Winer, J., Armanini, M., Cairns, B., Winslow, J., Gao, W. and Phillips, H. S. 1999. Regulation of learning by EphA receptors: a protein targeting study. *J. Neurosci.* **19**: 9538–9549.

6. Goodman, J. H. and Gilbert, M. E. 2007. Modest thyroid hormone insufficiency during development induces a cellular malformation in the corpus callosum: a model of cortical dysplasia. *Endocrinology* **148**: 2593–2597.

7. Kobayashi, K., Akune, H., Sumida, K., Saito, K., Yoshioka, T. and Tsuji, R. 2009. Perinatal exposure to PTU decreases expression of Arc, Homer 1, Egr 1 and Kcna 1 in the rat cerebral cortex and hippocampus. *Brain Res.* **1264**: 24–32.

8. Lavado-Autric, R., Ausó, E., García-Velasco, J. V., Arufe Mdel, C., Escobar del Rey, F., Berbel, P. and Morreale de Escobar, G. 2003. Early maternal hypothyroxinemia alters histogenesis and cerebral cortex cytoarchitecture of the progeny. *J. Clin. Invest.* **111**: 954–957.

9. Lee, K-Y., Shibutani, M., Inoue, K., Kuroiwa, K., U, M., Woo, G-H. and Hirose, M. 2006. Methacarn fixation—Effects of tissue processing and storage conditions on detection of mRNAs and proteins in paraffin-embedded tissues. *Anal. Biochem.* **351**: 36–43.

10. Masutomi, N., Shibutani, M., Takagi, H., Uneyama, C., Takahashi, N. and Hirose, M. 2003. Impact of dietary exposure to methoxychlor, genistein, or diisononyl phthalate during the perinatal period on the development of the rat endocrine/reproductive systems in later life. *Toxicology* **192**: 149–170.

11. Mileusnic, D., Lee, J. M., Magnuson, D. J., Hejna, M. J., Krause, J. E., Lorens, J. B. and Lorens, S. A. 1999. Neurokinin-3 receptor distribution in rat and human brain: an immunohistochemical study. *Neuroscience* **89**: 1269–1290.

12. Montero-Pedrazuela, A., Venero, C., Lavado-Autric, R., Fernández-Lamo, I., García-Verdugo, J. M., Bernal, J. and Guadaño-Ferraz, A. 2006. Modulation of adult hippocampal neurogenesis by thyroid hormones: implications in depressive-like behavior. *Mol. Psychiatry* **11**: 361–371.

13. Nakamura, R., Teshima, R., Hachisuka, A., Sato, Y., Takagi, K., Nakamura, R., Woo, G-H., Shibutani, M. and Sawada, J. 2007. Effects of developmental hypothyroidism induced by maternal administration of methimazole or propylthiouracil on the immune system of rats. *Int. Immunopharmacol.* **7**: 1630–1638.

14. Nordquist, R. E., Durkin, S., Jacquet, A. and Spooren, W. 2008. The tachykinin NK3 receptor agonist senktide induces locomotor activity in male Mongolian gerbils. *Eur. J. Pharmacol.* **600**: 87–92.

15. Numachi, Y., Yoshida, S., Yamashita, M., Fujiyama, K., Toda, S., Matsuoka, H., Kajii, Y. and Nishikawa, T. 2007. Altered EphA5 mRNA expression in rat brain with a single methamphetamine treatment. *Neurosci. Lett.* **424**: 116–121.

16. Oh-Nishi, A., Saji, M., Furudate, S. I. and Suzuki, N. 2005. Dopamine D_2-like receptor function is converted from excitatory to inhibitory by thyroxine in the developmental hippocampus. *J. Neuroendocrinol.* **17**: 836–845.

17. Olivieri, G. and Miescher, G. C. 1999. Immunohistochemical localization of EphA5 in the adult human central nervous system. *J. Histochem. Cytochem.* **47**: 855–861.

18. Porterfield, S. P. 2000. Thyroidal dysfunction and environmental chemicals—Potential impact on brain development. *Environ. Health Perspect.* **108**: 433–438.

19. Royland, J. E., Parker, J. S. and Gilbert, M. E. 2008. A genomic analysis of subclinical hypothyroidism in hippocampus and neocortex of the developing rat brain. *J. Neuroendocrinol.* **20**: 1319–1338.

20. Salthun-Lassalle, B., Traver, S., Hirsch, E. C. and Michel, P. P. 2005. Substance P, neurokinins A and B, and synthetic tachykinin peptides protect mesencephalic dopaminergic neurons in culture via an activity-dependent mechanism. *Mol. Pharmacol.* **68**: 1214–1224.

21. Schoonover, C. M., Seibel, M. M., Jolson, D. M., Stack, M. J., Rahman, R. J., Jones, S. A., Mariash, C. N. and Anderson, G. W. 2004 Thyroid hormone regulates oligodendrocyte accumulation in developing rat brain white matter tracts. *Endocrinology* **145**: 5013–5020.

22. Shibutani, M., Uneyama, C., Miyazaki, K., Toyoda, K. and Hirose, M. 2000. Methacarn fixation: a novel tool for analysis of gene expressions in paraffin-embedded tissue specimens. *Lab. Invest.* **80**: 199–208.

23. Shibutani, M., Lee, K-Y., Igarashi, K., Woo, G-H., Inoue, K., Nishimura, T. and Hirose, M. 2007. Hypothalamus region-specific global gene expression profiling in early stages of central endocrine disruption in rat neonates injected with estradiol benzoate or flutamide. *Dev. Neurobiol.* **67**: 253–269.

24. Shibutani, M., Woo, G-H., Fujimoto, H., Saegusa, Y., Takahashi, M., Inoue, K., Hirose, M. and Nishikawa, A. 2009. Assessment of developmental effects of hypothyroidism in rats from in utero and lactation exposure to anti-thyroid agents. *Reprod. Toxicol.* **28**: 297–307.

25. Smith, P. W. and Dawson, L. A. 2008. Neurokinin 3 (NK3) receptor modulators for the treatment of psychiatric disorders. *Recent Pat. CNS Drug Discov.* **3**: 1–15.

26. Takagi, H., Shibutani, M., Kato, N., Fujita, H., Lee, K-Y., Takigami, S., Mitsumori, K. and Hirose, M. 2004. Microdissected region-specific gene expression analysis with methacarn-fixed, paraffin-embedded tissues by real-time RT-PCR. *J. Histochem. Cytochem.* **52**: 903–913.

27. Uneyama, C., Shibutani, M., Masutomi, N., Takagi, H. and Hirose, M. 2002. Methacarn fixation for genomic DNA analysis in microdissected, paraffin-embedded tissue specimens. *J. Histochem. Cytochem.* **50**: 1237–1245.

28. Woo, G-H., Takahashi, M., Inoue, K., Fujimoto, H., Igarashi, K., Kanno, J., Hirose, M., Nishikawa, A. and Shibutani, M. 2009. Cellular distributions of molecules with altered expression specific to thyroid proliferative lesions developing in a rat thyroid carcinogenesis model. *Cancer Sci.* **100**: 617–625.